An Actin-binding Protein of the Sla2/Huntingtin Interacting Protein 1 Family Is a Novel Component of Clathrin-coated Pits and Vesicles

Åsa E.Y. Engqvist-Goldstein,* Michael M. Kessels,* Vikramjit S. Chopra,‡ Michael R. Hayden,‡ and David G. Drubin*

*Department of Molecular and Cell Biology, University of California, Berkeley, Berkeley, California 94720-3202; and ‡Centre for Molecular Medicine and Therapeutics, Department of Medical Genetics, Children's and Women's Hospital, University of British Columbia, Vancouver, British Columbia, Canada V5Z 4H4

Abstract. The actin cytoskeleton has been implicated in endocytosis, yet few molecules that link these systems have been identified. Here, we have cloned and characterized mHip1R, a protein that is closely related to huntingtin interacting protein 1 (Hip1). These two proteins are mammalian homologues of Sla2p, an actin-binding protein important for actin organization and endocytosis in yeast. Sequence alignments and secondary structure predictions verified that mHip1R belongs to the Sla2 protein family. Thus, mHip1R contains an NH_2-terminal domain homologous to that implicated in Sla2p's endocytic function, three predicted coiled–coils, a leucine zipper, and a talin-like actin-binding domain at the COOH terminus. The talin-like domain of mHip1R binds to F-actin in vitro and colocalizes with F-actin in vivo, indicating that this activity has been conserved from yeast to mammals. mHip1R shows a punctate immunolocalization and is enriched at the cell cortex and in the perinuclear region. We concluded that the cortical localization represents endocytic compartments, because mHip1R colocalizes with clathrin, AP-2, and endocytosed transferrin, and because mHip1R fractionates biochemically with clathrin-coated vesicles. Time-lapse video microscopy of mHip1R–green fluorescence protein (GFP) revealed a blinking behavior similar to that reported for GFP-clathrin, and an actin-dependent inward movement of punctate structures from the cell periphery. These data show that mHip1R is a component of clathrin-coated pits and vesicles and suggest that it might link the endocytic machinery to the actin cytoskeleton.

Key words: actin • endocytosis • clathrin • Huntington disease • vesicle

ENDOCYTOSIS is important for receptor internalization, nutrient uptake, antigen presentation, pathogen internalization, and maintenance of plasma membrane surface area (for reviews see Riezman et al., 1997; Marsh and McMahon, 1999). Endocytosis occurs via several distinct pathways and requires coordinated interactions between a variety of molecules at the cell cortex. In yeast, a functional connection between the actin cytoskeleton and endocytosis has been firmly established (for reviews see Geli and Riezman, 1998; Wendland et al., 1998). Mutations in actin and in several actin-binding proteins inhibit the internalization step of both receptor-mediated and fluid-phase endocytosis (Kübler and Riezman, 1993; Raths et al., 1993; Munn et al., 1995). Furthermore, studies using actin mutants and cofilin mutants suggest that rapid actin filament turnover is required for endocytosis (Lappalainen and Drubin, 1997; Belmont and Drubin, 1998). In mammalian cells, a role for actin in endocytosis has not been as clearly established. Cytochalasin-D, a drug that destabilizes actin filaments, inhibits apical endocytosis in polarized epithelial cells but has no effect on basolateral endocytosis (Gottlieb et al., 1993; Jackman et al., 1994). In other cell types, there are conflicting results on the effects of various actin-depolymerizing drugs on receptor-mediated endocytosis (Salisbury et al., 1980; Wolkoff et al., 1984; Sandvig and van Deurs, 1990; Lamaze et al., 1996, 1997).

Several functional roles for actin in endocytic processes have been proposed. The actin cytoskeleton might provide a force for vesicle budding, or it might mediate vesicle transport or fusion (Gottlieb et al., 1993; Lamaze et al., 1997; Merrifield et al., 1999). Alternatively, it might provide a scaffold at the plasma membrane for the endocytic machinery (Wendland et al., 1998; Gaidarov et al., 1999).

To gain further insight into the role of the actin cytoskeleton in endocytosis, it is important to identify proteins that link the actin cytoskeleton to the endocytic machin-

ery. In yeast, mutations of several actin-binding proteins cause defects in both endocytosis and in the organization of the actin cytoskeleton. One such protein is Sla2p, which was first identified in a synthetic lethal screen against a null allele of *ABP1* (Holtzman et al., 1993), a gene encoding an actin-binding protein implicated in cytoskeletal regulation, endocytosis, and cAMP signaling (Drubin et al., 1988; Wesp et al., 1997). Sla2p, also known as End4p and Mop2p, is a peripheral membrane protein that contains a novel NH$_2$-terminal domain, three putative coiled–coil domains, a putative leucine zipper, and a COOH-terminal talin-like domain (Holtzman et al., 1993; Raths et al., 1993; Na et al., 1995; Wesp et al., 1997; Yang et al., 1999). Sla2p binds to F-actin in vitro through the talin-like domain and partially colocalizes with F-actin in cortical patches (McCann and Craig, 1997; Yang et al., 1999). Interestingly, Sla2p localizes to the cell cortex in the presence of latrunculin-A (LAT-A),[1] indicating that Sla2p has an actin-independent cortical localization signal (Ayscough et al., 1997). Sla2p has been implicated in endocytosis (Raths et al., 1993), membrane protein maintenance (Na et al., 1995), and vesicle trafficking (Mulholland et al., 1997).

Homologues of Sla2p have been identified in nematodes (*ZK370.3*) and humans (Hip1R) (Holtzman et al., 1993; Seki et al., 1998), but very little is known about their cellular functions. In mammals, an additional isoform exists, the huntingtin interacting protein 1 (Hip1), which is predominantly expressed in the brain (Kalchman et al., 1997; Wanker et al., 1997). Huntington disease is an inherited neurodegenerative disorder caused by expansion of the codon CAG in the huntingtin gene, which leads to expression of a polyglutamine tract in the protein (for reviews see Wellington et al., 1997; Reddy et al., 1999). The affinity of the huntingtin protein–Hip1 interaction is inversely correlated to the polyglutamine length. Therefore, it has been speculated that loss of normal huntingtin–Hip1 interaction might contribute to a defect in membrane–cytoskeletal integrity in the brain (Kalchman et al., 1997). To learn more about the cellular function of the Sla2 family of proteins, we have initiated a study of the mouse homologue of Hip1R.

Materials and Methods

Cloning of mHip1R

A mouse brain lambda ZAPII cDNA library (#936314; Stratagene) was screened using a mouse expressed sequence tag (EST) obtained from American Tissue Culture Collection (ESTm1; sequence data available from EMBL/GenBank/DDBJ under accession no. W82687). 50 ng of a 1.3-kb EcoRI/NcoI fragment of this EST was radioactively labeled with [^{32}P]dCTP using random-priming. The probe was allowed to hybridize to filters containing $>2 \times 10^5$ pfu/ml of the mouse brain lambda ZAPII cDNA library, and incubated overnight at 65°C in Church buffer (0.5 M NaPO$_4$, 7% SDS, 1 mM EDTA, pH 7.4). The filters were washed at room temperature for 15 min with 2× SSPE (200 mM NaH$_2$PO$_4$, 3 M NaCl, 25 mM EDTA, pH 7.4) containing 0.1% SDS, then at 65°C for 20 min with 1× SSPE (200 mM NaH$_2$PO$_4$, 3 M NaCl, 25 mM EDTA, pH 7.4), containing 0.1% SDS, and finally twice at 65°C with 0.2× SSPE, containing 0.1% SDS. The filters were exposed to X-ray film overnight at −70°C. Primary positives were isolated, replated, and subsequent secondary positives were

---

1. *Abbreviations used in this paper:* aa, amino acid(s); EST, expressed sequence tag; GFP, green fluorescence protein; GST, glutathione *S*-transferase; Hip1, huntingtin interacting protein 1; LAT-A, latrunculin-A.

hybridized and washed as for the primary screen. The resulting positive phage was converted into plasmid DNA by conventional methods (Stratagene) and the cDNA (3.96 kb) encoding mHip1R was isolated and completely sequenced.

DNA Constructions

Two murine ESTs were obtained from American Tissue Culture Collection, ESTm1 and ESTm2 (sequence data available from EMBL/GenBank/DDBJ under accession nos. W82687 and AA10840, respectively). The plasmid DNA was isolated and sequenced. These EST clones and the full-length mHip1R cDNA (see above) were used to generate the different constructs in this study.

For the antibody production and for in vitro actin-binding assays, fragments of mHip1R were expressed as glutathione *S*-transferase (GST) fusion proteins in *E. coli*. mHip1R (amino acids [aa] 1015–1068) was amplified by PCR using primers that generate NcoI and EcoRI sites at the 5′ and 3′ ends, respectively. mHip1R (aa 766–1068) was amplified using primers that generate XhoI and HindIII sites at the 5′ and 3′ ends, respectively. The PCR products were cut with the above restriction enzymes and ligated into the pGAT2 vector (a GST fusion derivative of pBAT; Peränen et al., 1996).

For expression of mHip1R constructs in mammalian cells, full-length protein (aa 1–1068) and fragments of mHip1R were expressed as green fluorescence protein (GFP) fusions, or were expressed with a 6 myc-tag at the COOH terminus. mHip1R (aa 1–1068)–GFP and mHip1R (aa 1–324)–GFP were amplified by PCR using primers that generate NheI and SalI sites at the 5′ and 3′ ends, respectively. The PCR products were ligated into pEGFP-N1 (Clontech, Inc.). The linker region created between mHip1R and GFP consists of the 14 aa QSTVPRARDPPVAT. mHip1R (aa 1–1068)–GFP, mHip1R (aa 346–1068)–GFP, and mHip1R (aa 766–1068)–GFP were amplified by PCR using primers that generate XhoI and XbaI sites at the 5′ and 3′ ends, respectively. The PCR products were ligated into pEGFP-C1 (Clontech, Inc.). A linker region of 10 aa (SGL-RSRAGGS) was created between GFP and mHip1R. mHip1R (aa 1–1068)–6 myc, mHip1R (aa 1–324)–6 myc, mHip1R (aa 1–655)–6 myc, mHip1R (aa 346–1068)–6 myc, and mHip1R (aa 766–1068)–6 myc were amplified by PCR using primers that generate ClaI and NotI sites at the 5′ and 3′ ends, respectively. The PCR products were ligated into a 6 myc derivative of pIRESneo (Clontech, Inc.). This vector was created by cloning a 6 myc-tag into the Not1 and BamH1 sites of the pIRESneo vector. This created a linker region between the mHip1R sequence and the 6 myc-tag consisting of 5 aa (SRPQAM). A Kozac site including the ATG was added to constructs that do not contain the NH$_2$ terminus. All constructs were sequenced to ensure that no mutations were introduced during PCR. In addition, all constructs were tested for expression by Western blotting (see below).

Northern Blot Analysis of mHip1R mRNA

Northern blot analyses of mHip1R mRNA levels were performed using blots containing either 2 μg RNA per lane from eight different tissues or RNA from mouse embryos at four different embryonic stages (Clontech, Inc.). A 297-bp DNA fragment corresponding to mHip1R (aa 970–1068) was amplified by PCR using ESTm1 as a template. To generate a probe, this DNA fragment was labeled with [α-^{32}P]CTP (Amersham Pharmacia Biotech) using an oligonucleotide labeling kit which employs Klenow polymerase (Amersham Pharmacia Biotech). Unincorporated nucleotides were removed using MicroSpin S-200 columns (Amersham Pharmacia Biotech). 37.5 ng of the labeled probe (sp act = 8×10^5 cpm/ng) were used per blot. The blots were prehybridized in ExpressHyb solution (Clontech, Inc.) for 30 min at 68°C. The probe was then added to the prehybridized blots and incubated at 68°C for 1.5 h. The blots were then washed at room temperature three times for 1 min and three times for 10 min in 300 mM NaCl, 30 mM sodium citrate, pH 7.0, containing 0.05% SDS, and were subsequently washed at 50°C twice for 20 min with prewarmed 15 mM NaCl, 1.5 mM sodium citrate, pH 7.0, containing 0.1% SDS. mHip1R mRNAs were detected by exposing the blots for 7–8 d on autoradiography film. A probe derived from a human β-actin cDNA (Clontech, Inc.) was used to control for RNA loading and integrity. Blots were reused after stripping them in 0.5% SDS at 90–100°C for 10 min under frequent rocking. Completion of stripping was verified by autoradiography.

Production of Polyclonal Anti-mHip1R Antibodies

Polyclonal guinea pig antisera were raised against a nonconserved region

at the COOH terminus of mHip1R (aa 1032–1068). mHip1R (aa 1015–1068) was expressed as a GST fusion in *E. coli*. The protein was purified using glutathione–affinity chromatography, cleaved with thrombin (Sigma Chemical Co.) and purified by gel filtration followed by HPLC. This procedure yielded a degradation product of high purity (aa 1032–1068, as identified by mass spectrometry). This polypeptide was then conjugated to guinea pig albumin and mixed with Ribi adjuvant (R-700; Ribi Immunochem Research, Inc.) for injection into Hartley guinea pigs (100 μg protein per injection). After the initial injection, boosts were given every 3–4 wk. The crude sera were screened against 0.5–500 ng of purified mHip1R (aa 765–1068) and against mouse tissue homogenates by immunoblotting. After five injections, the crude antiserum was purified by affinity chromatograpy as described by Kozminski et al. (2000). In brief, mHip1R (aa 1015–1068)–GST was conjugated to Reacti-Gel™ (Pierce) following the manufacturer's instructions, and poured into a column. The column was washed and the crude serum was circulated through the column overnight. After extensive washing, the antiserum was eluted with 0.05 M Tris-HCl, 4.5 M MgCl$_2$, 1 mg/ml BSA, pH 7.4. This antibody is referred to as GP#8.

Immunoblot Analysis of mHip1R

Tissues for Western blotting were harvested from adult female Swiss Webster mice and immediately frozen in liquid nitrogen. The different tissues and organs were minced using a razor blade, and homogenized at 4°C using a dounce glass homogenizer (size AA; $\sim$20 strokes). For homogenization, 3 ml/g tissue homogenization buffer A (250 mM sucrose, 10 mM EGTA, 2 mM EDTA, 20 mM Tris, pH 7.5) containing a protease inhibitor cocktail (10 μg/ml leupeptin, 10 μg/ml aprotinin, 10 μg/ml soybean trypsin inhibitors, and 1 mM PMSF) was used. The samples were centrifuged at 4°C for 20 min at 4,000 rpm in a microcentrifuge. The resulting supernatants were used for Western blot analysis, in which equal amounts of protein were loaded in each lane.

Cell line homogenates were prepared by growing cells to confluence, rinsing the cells with ice-cold PBS, scraping the cells off the plates, collecting them by centrifugation, and lysing the cell pellets in ice cold homogenization B (150 mM NaCl, 2 mM EDTA, 1% NP-40, 50 mM Hepes, pH 7.5) supplemented with the protease inhibitor cocktail A at 350 μl/5 $\times$ 10^6 cells. The crude homogenate was then dounced as described above, and spun for 5 min at 5,000 rpm at 4°C in a microcentrifuge.

SDS-PAGE was performed and proteins were transferred to nitrocellulose membranes in transfer buffer containing 0.05% SDS. Membranes were then blocked for 1.5 h with TBS/0.05% Tween 20 containing 5% nonfat milk, followed by incubation with affinity-purified anti-mHip1R antiserum. The primary antibodies were visualized using HRP-conjugated anti–guinea pig secondary antibodies (ICN Pharmaceuticals, Inc.) and enhanced chemiluminescence (Amersham Pharmacia Biotech).

In Vitro Actin-binding Assay

The talin-like domain of mHip1R (aa 766–1068) was expressed as a GST fusion in *E. coli* Bl21 (DE3) cells using the pGAT2 plasmid constructs described above. Cultures were grown to OD$_{600}$ = 0.5 and expression was induced by addition of 0.4 mM isopropyl-thio-β-D-galactoside (IPTG; Sigma Chemical Co.). Cells were lysed by one freeze–thaw cycle, followed by sonication (six times for 20 s) in PBS containing 10 mM EGTA and 0.5 mM PMSF. The GST fusion protein was purified using glutathione–affinity chromatography as described by Ausubel et al. (1994). The purified GST–talin-like domain was then used in an actin filament cosedimentation assay. Actin filaments were assembled as described by Goode et al. (1999) with minor alterations. In brief, 0.1 vol of 10$\times$ initiation mix (20 mM MgCl$_2$, 0.5 M KCl, 5 mM ATP) was added to human nonmuscle monomeric actin (Cytoskeleton) in G-buffer (5 mM Tris, pH 7.5, 0.2 mM ATP, 0.2 mM DTT, and 0.2 mM CaCl$_2$), and was then incubated for 30 min at 20°C. The cosedimentation assays were performed using 50-μl reactions containing 1.25–10 μM α-actin and 1.5 μM GST–talin-like domain. The mixtures were centrifuged for 25 min at 90,000 rpm at 20°C in a TLA100 rotor (Beckman). Pellets and supernatants were resuspended in SDS sample buffer and equal volumes were analyzed by SDS-PAGE, followed by Coomassie blue staining. Protein amounts was quantified using an IS-100 densitometer (Alpha Innotech Corp.).

Cell Culture

NIH/3T3, COS-7, and MDCK cells were maintained in DME (GIBCO BRL) containing 10% FBS.

Indirect Immunofluorescence

Cells grown on glass coverslips were washed with 50 mM MES, pH 6.1, 5 mM MgCl$_2$, 3 mM EGTA, 5 mM glucose, and were then incubated with 3–4% formaldehyde, 0.1% glutaraldehyde in the same buffer for 35–45 min. The fixed cells were quenched with 1 mg/ml NaBH$_4$ (twice for 10 min) to prevent autofluorescence, and then blocked and permeabilized with TBS (20 mM Tris, pH 7.5, 154 mM NaCl, 2 mM EGTA, 2 mM MgCl$_2$) containing 2% BSA and 0.02% saponin for 1.5 h. The coverslips were then incubated on 20-μl droplets of primary antibody diluted in TBS/BSA/saponin overnight. The following primary antibodies were used: polyclonal anti-GFP antibody (kindly provided by Dr. Pam Silver, Dana Farber Cancer Institute, Harvard Medical School, Boston, MA); polyclonal anti-mHip1R (see above); monoclonal anti–AP-2 antibody (AP-6) and monoclonal anticlathrin antibody (X22) (Affinity Bioreagents); monoclonal anticlathrin antibody (Transduction Laboratories); monoclonal anti-paxillin antibody (Transduction Laboratories); polyclonal anti-Abp1 antibody (Kessels et al., 2000); and monoclonal anti-myc antibody 9E10 (Santa Cruz Biotechnology). After incubation with the primary antibodies, the coverslips were washed three times for 15 min with TBS/BSA/saponin, and incubated with the secondary antibodies in TBS/BSA/saponin for 1.5 h. The following secondary antibodies were used: FITC goat anti–guinea pig (ICN Pharmaceuticals, Inc.); rhodamine goat anti–guinea pig (ICN Pharmaceuticals, Inc.); FITC donkey anti–mouse (Jackson ImmunoResearch Laboratories); rhodamine donkey anti–mouse (Jackson ImmunoResearch Laboratories); FITC goat anti–rabbit (ICN Pharmaceuticals, Inc.); and rhodamine sheep anti–rabbit (Cappel), and/or rhodamine-phalloidin (Molecular Probes). After incubation in secondary antibodies, the coverslips were washed in TBS/BSA/saponin (15 min) and with TBS (twice for 15 min). After removing excess buffer, the coverslips were mounted onto glass slides using VectaShield mounting medium containing 4,6-diamidino-2-phenylindole dihydrochloride (Vector, Inc.), sealed with nail polish, and viewed using an inverted Nikon Eclipse TE300 fluorescence microscope or with a Zeiss 510 confocal laser scanning microscope. For epifluorescence microscopy, images were captured using a cooled CCD Hamamatsu ORCA camera and were recorded digitally (ImageProPlus; Phase3 Imaging Systems). For confocal microscopy, images were captured using Zeiss 510 software. All images were prepared for publication using Adobe Photoshop software.

Transferrin Uptake Assay

COS-7 cells grown on glass coverslips were serum starved for 45 min at 37°C in DME. Cells were then incubated with 25 μg/ml human transferrin conjugated to Texas red (Molecular Probes) in serum-free media for 1 h at 4°C. Subsequently, the coverslips were washed three times for 5 min with ice-cold PBS, and then fixed with an ice-cold solution of 4% formaldehyde and 0.1% glutaraldehyde (0 min) or warmed to 37°C for 2, 5, 10, 15, or 30 min before they were washed and fixed as described above. The fixed cells were then incubated with anti-mHip1R antibody, followed by FITC anti–guinea pig antibody and were examined by confocal microscopy as described above.

Transfection of COS-7 Cells with mHip1R Constructs

First, the expression of GFP fusion proteins and myc-tagged proteins was verified by immunoblotting. Cells were plated at 300,000 cells/well (6-well plates) on glass coverslips, 24 h before transfection. Transfections were performed using the lipofectamine method according to the manufacturer (GIBCO BRL). Typically, 1 μg of DNA per 1 ml transfection medium was used, and transfections were performed for 5 h at 37°C. The solution was then replaced by complete medium (DME containing 10% FBS) and cells were harvested 48 h after transfection. Homogenization buffer (see above) containing 1% Triton X-100 was added directly to the 6-well plates and cells were scraped off and homogenized using a 25-gauge needle. Cells were then centrifuged at 15,000 rpm for 20 min at 4°C in a microcentrifuge. The resulting pellets and supernatants were analyzed by immunoblotting using polyclonal anti-GFP antibodies or monoclonal anti-myc antibodies.

Second, subcellular localization of GFP fusion proteins and myc-tagged proteins was determined by indirect immunofluorescence. Cells were transfected as described above and processed for immunofluorescence 24–36 h after transfection as described above. Constructs used in these experiments are described above.

Subcellular Fractionation and Purification of Clathrin-coated Vesicles

For subcellular fractionation, 0.7–0.8 g of mouse brain was homogenized in homogenization buffer A (250 mM sucrose, 10 mM EGTA, 2 mM EDTA, 20 mM Tris, pH 7.5) containing the protease inhibitor cocktail A (1:1 wt/vol) and spun at 3,000 g for 20 min. P1 contains unbroken cells, nuclei, mitochondria, and large plasma membrane pieces. The supernatants (S1) were collected and spun at 25,000 g for 30 min to generate P2 (small plasma membrane pieces, ER, and endosomes) and S2. Supernatant S2 was spun at 176,000 g for 1 h to generate P3 (light microsomes and small vesicles) and S3 (soluble proteins). For extraction experiments, P2 was resuspended in homogenization buffer A containing either 1% Triton X-100 or 0.5 M NaCl. After incubation on ice for 30 min, the fractions were spun at 25,000 g for 30 min. The protein concentration of each fraction was determined by the Bradford method (1976). Equal amounts of protein were examined by SDS-PAGE and immunoblotting.

Purification of clathrin-coated vesicles was performed as described by Lindner (1998) with minor alterations. In brief, 10 mouse brains (~5 g)

(Pel Freez Biologicals) were minced using a razor blade and homogenized in 5 ml buffer C (0.1 M MES, 1.0 mM EGTA, 0.5 mM MgCl₂, pH 6.5) containing the protease inhibitor cocktail A. Postmitochondrial supernatants (S1) were spun at 120,000 g in a Type70 rotor (Beckman) for 50 min at 4°C to prepare a microsomal pellet (P2). P2 was resuspended in 0.4 ml buffer C containing the protease inhibitor cocktail A and homogenized by 10–15 strokes in a Potter-Elvehjem device. The resuspended P2 was mixed with 0.4 ml 12.5% ficoll–sucrose solution and spun at 43,000 g in a TLA100.3 rotor (Beckman) for 40 min at 4°C. The resulting supernatant (S3) was mixed with 1.8 ml buffer C containing the protease inhibitor cocktail A and subsequently spun at 125,000 g in a TLA100.3 rotor for 30 min at 4°C. The pellet (V), which contains the enriched clathrin-coated vesicles, was resuspended in 100 μl buffer C. The S4 fraction was TCA-precipitated and resuspended in the same volume as the pellet (V). Samples were analyzed by SDS-PAGE followed by Coomassie blue staining and by Western blotting as described above. Equivalent portions of P1, S1, P2, and S2, corresponding to ~0.02% of each fraction, were loaded on the gel. For S3, P3, S4, and V, equivalent portions corresponding to ~2% of the fraction were loaded.

Figure 1. Analysis of mHip1R sequence. (a) Comparison of the full-length aa sequence identities of Sla2-related proteins. The percentage identity for the two most similar proteins is highlighted in bold. For hHip1R, the cDNA sequence reported by Ishikawa et al. (1998) was used (KIAA0655 protein; sequence data available from EMBL/GenBank/DDBJ under accession no. AB014555). (b) Sequence alignment of the NH₂-terminal domain in Sla2-related proteins. Residues that are conserved in at least four proteins are boxed. For hHip1R, residue M179, designated as the first methionine by Seki et al. (1998), is highlighted in bold. The upstream hHip1R sequence is from Ishikawa et al. (1998). The hHip1 sequence displayed represents a sequence published by Kalchman et al. (1997) (M82-A277), and a recently identified upstream sequence (S1-D81) (Chopra, V.S., unpublished results). (c) Schematic diagram showing mHip1R domain organization. The three predicted coiled–coil forming domains and the leucine zipper are indicated, as well as the COOH-terminal talin-like domain, and the NH₂-terminal domain. The Coils program (Lupas et al., 1991) was used to determine the probability of coiled–coil formation.

The following antibodies were used in the above experiments: polyclonal anti–amphiphysin II antibody (kindly provided by Harvey T. McMahon, Medical Research Council Laboratories, Cambridge, UK); polyclonal anti-mHip1R antibody; monoclonal anticlathrin antibody (Transduction Laboratories); monoclonal antipaxillin antibody (Transduction Laboratories); polyclonal anti-Abp1 antibody; polyclonal eps15 antibody (Santa Cruz Biotechnologies); monoclonal antiactin antibody C4 (ICN Pharmaceuticals, Inc.); polyclonal anti-BiP 1 (StressGen Biotech Corp.); and monoclonal anti-syntaxin 1 (Sigma Chemical Co.).

Imaging of mHip1R-GFP in Living Cells

NIH/3T3 fibroblasts were transfected with mHip1R (aa 1–1068)–GFP as described above. The coverslips were transferred to F-12 media (GIBCO BRL) containing 5% FCS and 10 mM Hepes, pH 7.4. Cells expressing low to medium levels of GFP fusion protein were imaged using an inverted Nikon Eclipse TE300 fluorescence microscope with a Nikon Plan Apo (1.4 NA) 100× objective and a Hamamatsu ORCA cooled CCD camera. GFP fluorescence was visualized with 1.5–20 s exposures using a B-2E/C (FITC) filter set (Nikon). During the experiments, the coverslips were maintained at 37°C using an aluminum chamber connected to a circulating water bath. The light was shuttered to reduce photobleaching when exposure times were >2 s. For observation of LAT-A treatments, media containing 2 μM LAT-A were added to the chamber. For observation of detergent-extracted cells, 0.05 vol of Triton X-100 (20% vol/vol) were added to cells at frame 5–10 of continuous time-lapse recording (1.5 s per frame) and observed for ~1 min.

Results

Identification and Sequence Analysis of a Mouse Homologue of Yeast Sla2p

To identify mammalian homologues of yeast Sla2p, we performed a database search. Several EST clones from mouse and human were identified that encoded either Hip1 or a novel protein related to Hip1. Different EST clones for this novel protein were obtained and sequenced. ESTm1 was used to screen a mouse brain lambda ZAPII cDNA library, and an ~4 kb cDNA was subsequently identified. This cDNA contains a 3,204-kb open reading frame predicted to encode a 119.5-kD protein (1068 aa).

Sequence alignments of this open reading frame with other Sla2-related proteins from different organisms revealed that it is highly homologous (91% identity over the entire aa sequence) to the recently identified protein Hip1R (human Hip1-related; Seki et al., 1998) (Fig. 1 a). Because of the high identity and the similarity in tissue distribution between these two proteins (see below), we believe that the novel Sla2-related protein we identified is
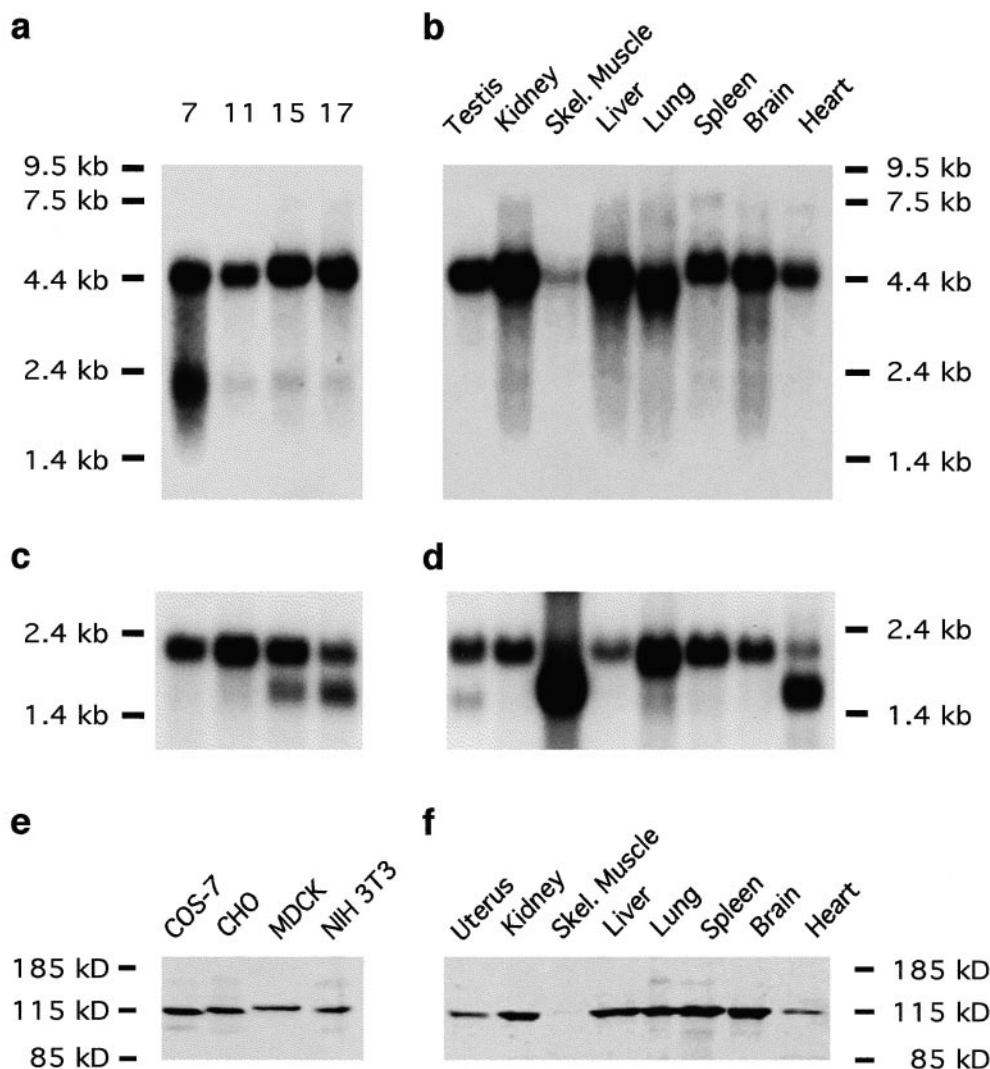
Figure 2. Mouse mHip1R mRNA and protein expression levels. (a) mHip1R mRNA expression examined by Northern blotting during the course of mouse embryonic development. The numbers at the top of each lane represent days after fertilization. (b) mHip1R mRNA expression in different tissues of adult mice. The Northern probe comprised 297 bp at the COOH terminus corresponding to aa 970–1068. (c and d) Actin expression is shown as a control for RNA integrity and loading. (e) mHip1R protein expression examined by Western blotting in different cell lines. Approximately 50 μg protein from postnuclear tissue homogenates was loaded per lane. (f) mHip1R protein expression in different adult mouse tissues. Approximately 200 μg of protein was loaded per lane.

the mouse ortholog of human Hip1R. Therefore, we decided to call it mHip1R. However, one major difference between these two proteins exists within the NH_2-terminal domain: Seki et al. (1998) selected a start codon ~180 aa downstream from the start codon we selected. It is likely that these aa are part of the translated coding sequence, because they show strong homology to the first half of the NH_2-terminal domain that is highly conserved among Sla2-related proteins (Fig. 1 b). mHip1R shows 24–60% identity to the other Sla2-related proteins in this domain. Additionally, we identified a Kozac translational initiation consensus sequence at the start codon that we favor. Finally, the human clone identified by Ishikawa et al. (1998) also contains the full NH_2-terminal domain. However, it remains possible that different spliced variants of Hip1R exists in humans, which may explain the truncation of the NH_2-terminal domain in hHip1R reported by Seki et al. (1998).

As shown in Fig. 1 c, the domain structure and predicted coiled–coil domains of mHip1R are similar to those of all other Sla2-related proteins. However, in contrast to Sla2p, mHip1R does not contain a proline-rich region or a glutamine-rich region. These regions also do not appear in Sla2-related proteins from nematodes, mice, or humans.

mHip1R Is Ubiquitously Expressed in Mouse Tissues

Northern blot analysis of mouse embryos showed that mHip1R mRNA levels do not change appreciably during development (Fig. 2 a). Furthermore, the mRNA is detected in all tissues tested, although the levels are lower in skeletal muscle and heart (Fig. 2 b). This is in contrast to hHip1 mRNA, which is highly enriched in the brain (Kalchman et al., 1997), but it is consistent with results from Ishikawa et al. (1998) and Seki et al. (1998), who showed by RT-PCR that hHip1R is expressed in a wide variety of human tissues. The size of the mHip1R mRNA was ~5 kb and varies slightly in different tissues (Fig. 2, a and b). In addition, an ~2-kb band was detected during the early stage of embryonic development (Fig. 2 a).

Polyclonal antibodies were raised against the extreme COOH terminus of mHip1R (aa 1032–1068), which is a region that is not conserved between any of the known Sla2-related proteins. Our affinity-purified antibody detected a band of ~120 kD in all cell lines and tissues tested on Western blots (Fig. 2, e and f). The mHip1R signal in skeletal muscle is extremely low (Fig. 2 f), which corresponds well with the mRNA levels detected by Northern blotting. Furthermore, the size of this protein corresponds to the molecular weight predicted for mHip1R. This band was not detected with preimmune serum or with anti-mHip1R sera preincubated with the antigen (data not shown).

The Talin-like Domain of mHip1R Binds F-Actin In Vitro

McCann and Craig (1997) showed that yeast Sla2p binds to F-actin in vitro through the talin-like domain. They named this domain the I/LWEQ module due to the presence of several conserved residues (McCann and Craig, 1997). To test whether this binding activity is conserved in mHip1R, the talin-like domain (aa 766–1068) was expressed in *E. coli* as a GST fusion and tested for actin binding in an F-actin pelleting assay (Fig. 3 a). Expression
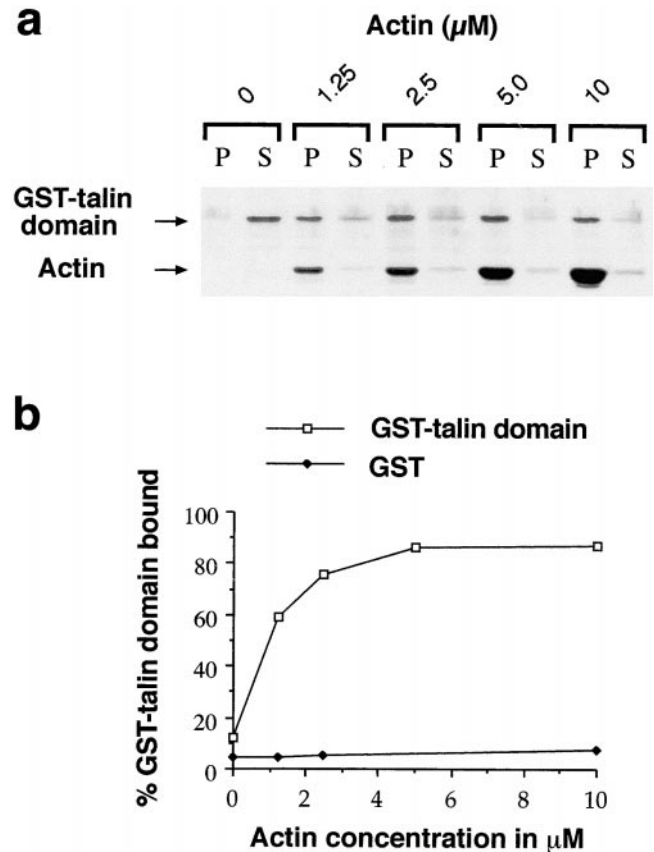
Figure 3. The talin-like domain of mHip1R binds to F-actin. (a) SDS-PAGE of a cosedimentation assay. The gels were stained with Coomassie blue, where P represents the pellets and S represents the supernatants. 0–10 μM nonmuscle actin was used with a constant concentration of GST-talin domain (1.5 μM). (b) Percentage of GST-talin domain bound to actin as a function of actin concentration. GST alone was used as a control. This experiment was repeated three times with similar results.

and solubility problems precluded the analysis of the full-length protein. As shown in Fig. 3 b, the talin-like domain of mHip1R binds to F-actin in a specific, saturable, and concentration-dependent manner with a relatively high affinity.

mHip1R Shows a Punctate Perinuclear and Cortical Subcellular Localization

The antibody raised against mHip1R (aa 1032–1068) was used to study its subcellular localization in different cell lines. This antibody labeled punctate structures that were enriched at the cell cortex and excluded from the nucleus (Fig. 4, a–f). The punctate subcellular distribution was observed in all cell lines examined (COS-7, NIH/3T3 fibroblasts, MDCK, and PC12). The mHip1R-positive staining is also enriched in the perinuclear region, where it often appears more continuous (Fig. 4 a and Fig. 5 d).

The cortical staining was present on all surfaces. Similar results were obtained with polarized MDCK cells, in which case the Hip1R staining was observed both on apical and basolateral surfaces (data not shown). At the cell
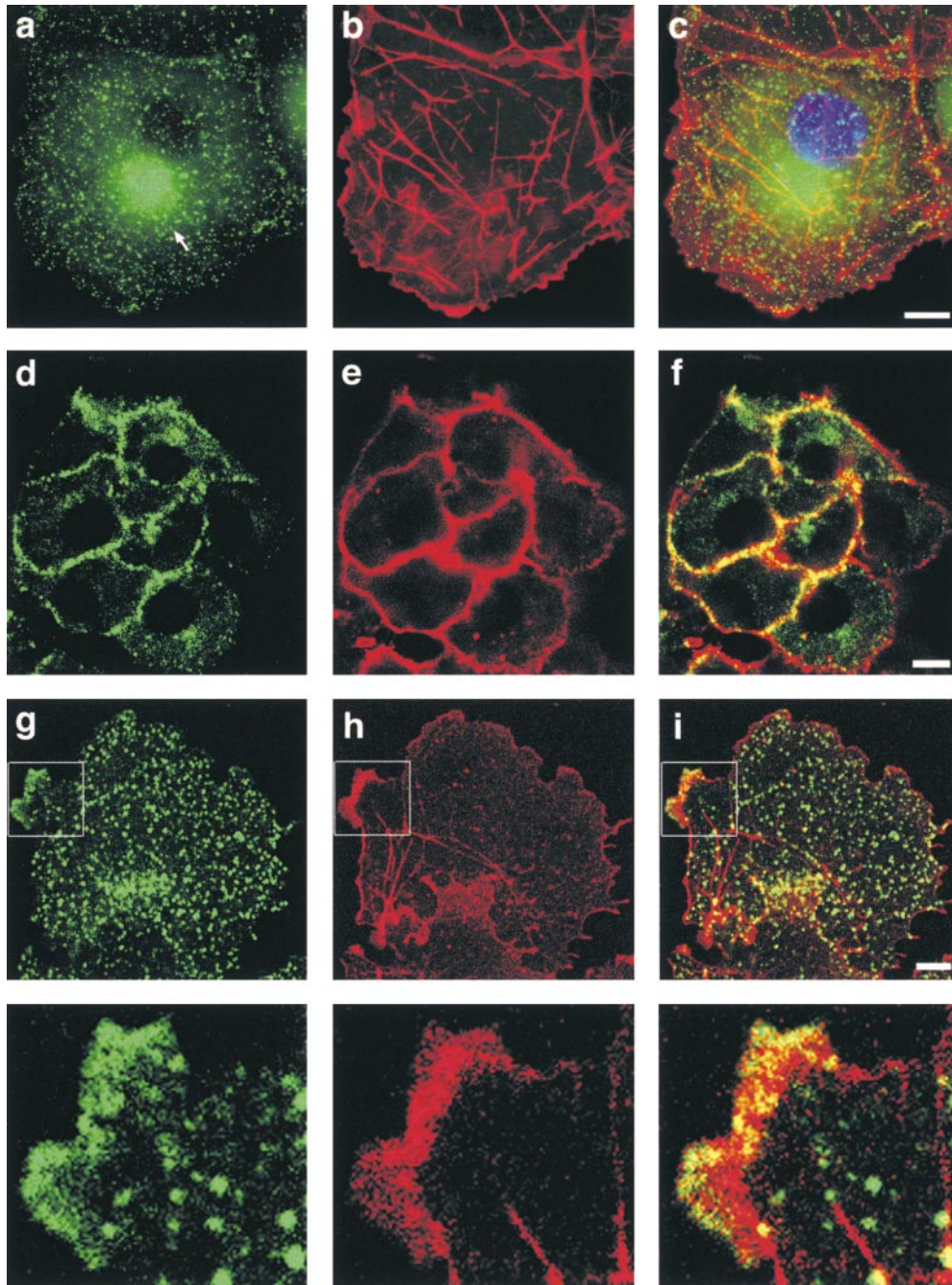
Figure 4. Indirect immuno-fluorescence of endogenous Hip1R in COS-7 cells. (a, d, and g) Labeling of Hip1R by GP#8 and anti–guinea pig FITC secondary antibody. (b, e, and h) F-actin staining labeled by rhodamine-phalloidin. (c, f, and i) Overlay between Hip1R and F-actin. In c this merge also includes 4,6-diamidino-2-phenylindole dihydrochloride staining to label the nucleus. Bars, 10 μM. (a–c) Punctate vesicle-like Hip1R localization that is enriched in the perinuclear area (a, arrow). (d–f) Hip1R-positive puncta are enriched at the actin-rich cell cortex as demonstrated by confocal microscopy sectioning through a medial plane of a clump of cells. (g–i and enlargements) Hip1R is present in some F-actin–rich ruffles, where the staining is less punctate and more continuous and colocalizes partially with F-actin. Confocal images close to the cell attachment surface.

periphery, Hip1R was also present in some F-actin–rich membrane ruffles, where the staining appeared continuous rather than punctate (Fig. 4, g–i). In these ruffles, Hip1R partially colocalized with F-actin (Fig. 4 i). Since mHip1R contains an actin-binding domain that is homologous to that of the focal adhesion protein talin, it was important to determine whether mHip1R also localizes to focal adhesions. However, double-labeling with paxillin, another focal adhesion protein, showed that mHip1R does not localize to focal adhesions (data not shown). In summary, mHip1R shows a punctate staining pattern and is enriched at the cell cortex and in the perinuclear region, and is present in some membrane ruffles.

mHip1R Colocalizes with Markers for Receptor-mediated Endocytosis

The yeast homologue of mHip1R (Sla2p) is required for endocytosis and localizes to cortical patches that partially overlap with actin patches. Because of the limited resolution in yeast cells, it has been difficult to determine whether Sla2p colocalizes with components of the endocytic machinery. To address this question in mammalian cells, we examined whether the punctate structures stained by the anti-mHip1R antibodies are also recognized by different markers for receptor-mediated endocytosis. We first tested whether mHip1R colocalizes with the coat protein, clathrin, which is involved in budding of vesicles from
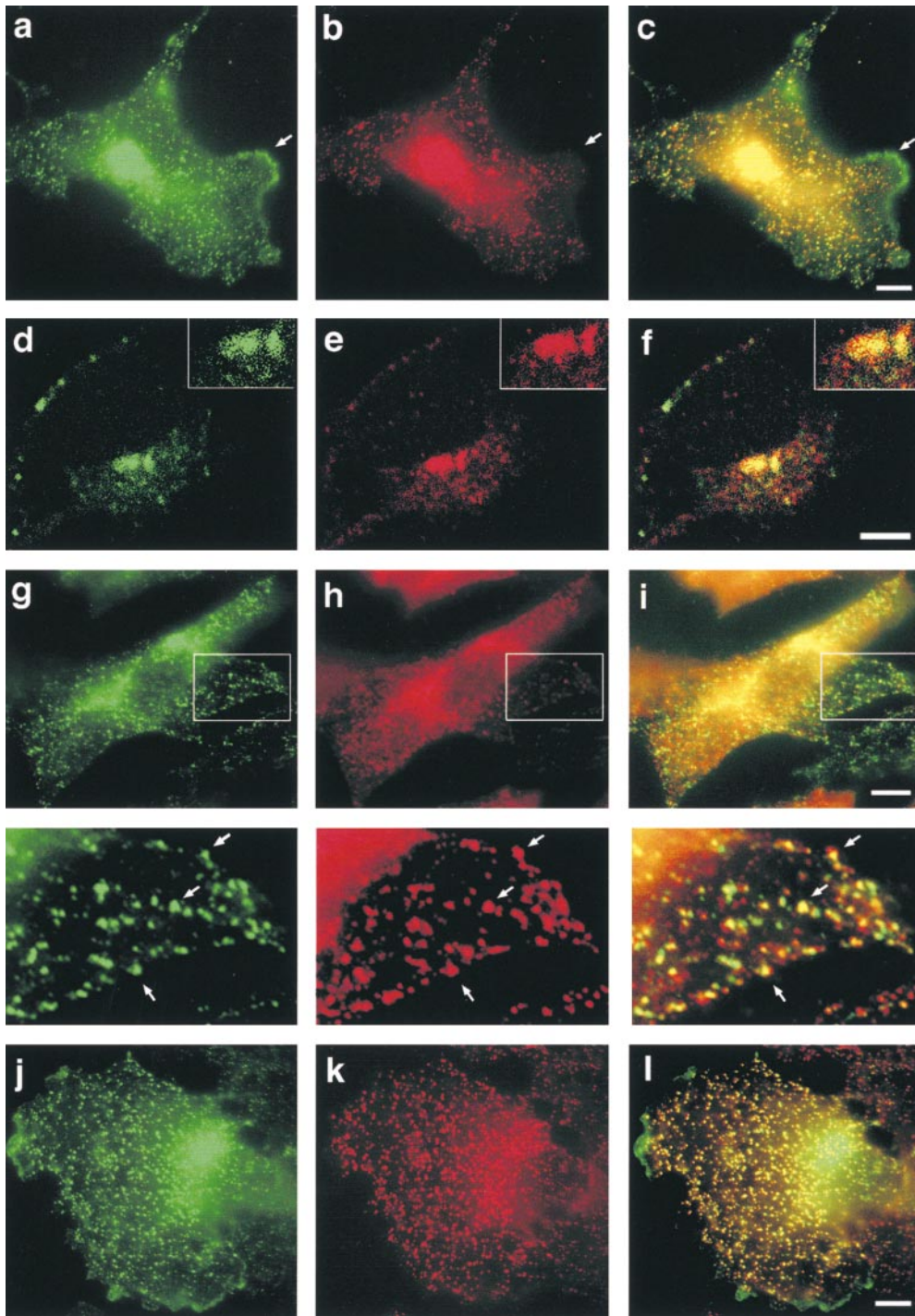
Figure 5. mHip1R colocalizes with clathrin and AP-2 in COS-7 and NIH/3T3 fibroblasts. (a, d, g, and j) mHip1R. (b, e, and h) Clathrin. (k) AP-2. (c, f, i, and l) Overlay. (a–c) COS-7 cells. mHip1R and clathrin show a similar subcellular distribution, including enrichments in the perinuclear areas. Bar, 10 μM. (d–f and insets) Confocal microscopy of COS-7 cells. mHip1R largely colocalizes with clathrin in the perinuclear region. Bar, 5 μM. (g–i and enlargements) NIH/3T3 cells. mHip1R partially colocalizes with clathrin at the cell cortex. Bar, 10 μM. (j–l) COS-7 cells. Colocalization of mHip1R and AP-2. Bar, 10 μM.

the plasma membrane and from the TGN (for review see Hirst and Robinson, 1998). mHip1R and clathrin showed an overall similar subcellular distribution and colocalization. Both are enriched in the perinuclear region (Fig. 5, a–c). The mHip1R and clathrin perinuclear colocalization is especially evident when examined by confocal microscopy (Fig. 5, d–f). Additionally, the cortical mHip1R and clathrin staining colocalized (Fig. 5, g–i). The only marked difference in the staining patterns of mHip1R and clathrin was in membrane ruffles, structures in which mHip1R, but not clathrin, is present (Fig. 5 a, arrow). We also tested

whether mHip1R colocalizes with the adaptor protein AP-2, which is involved in budding from the plasma membrane during clathrin-mediated endocytosis. As shown in Fig. 5, j–l, the staining pattern of mHip1R is almost identical to that of AP-2, except that AP-2 was not detected in the perinuclear region or in membrane ruffles.

Next, we tested whether Hip1R colocalizes with transferrin-labeled endosomal compartments in COS-7 cells. Pulse–chase experiments using Texas red–labeled transferrin showed that Hip1 partially colocalizes with endocytic compartments (Fig. 6). At 2–5 min uptake, trans-
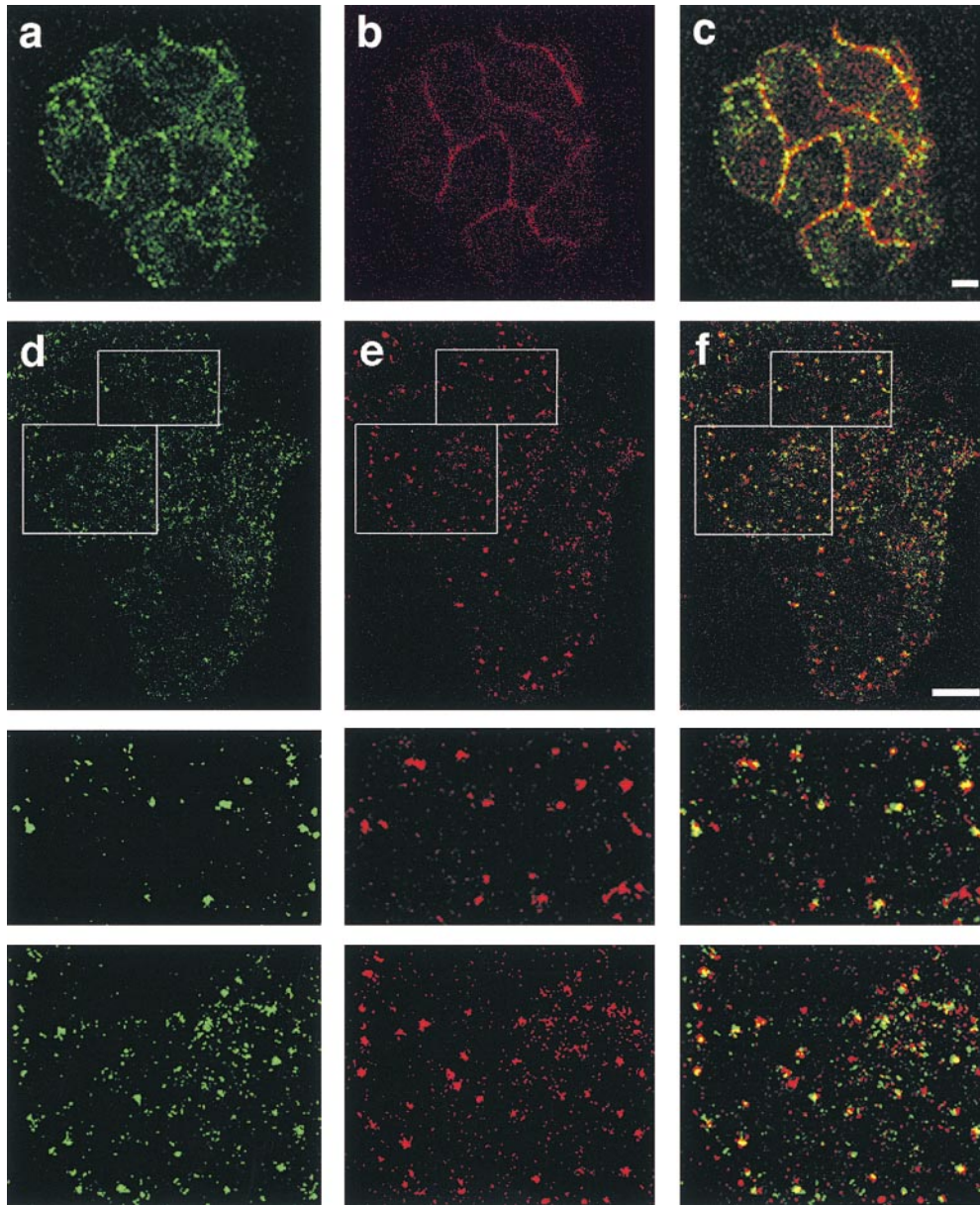
Figure 6. Hip1R partially colocalizes with transferrin-labeled endocytic compartment in COS-7 cells. (a and d) mHip1R. (b and e) Transferrin–Texas red. (c and f) Overlay. (a–c) At 2 min of uptake, transferrin labels the cell cortex (confocal medial section of cell clump). Hip1R-positive puncta overlaps with this cortical staining. (d–f and enlargements) At 10 min of transferrin uptake, Hip1R partially colocalizes with transferrin-labeled endocytic compartment. The confocal images are showing a section close to the attachment surface as observed by confocal microscopy. Bars, 10 μM.

ferrin shows a rather continuous labeling of the cell cortex, and it is difficult to discern any individual puncta (Fig. 6 b). Hip1R-positive puncta at the cell cortex overlap with this cortical transferrin staining (Fig. 6, a–c). After 5–15 min uptake, transferrin showed a punctate staining that partially colocalizes with Hip1R (Fig. 6, d–f). At later stages of uptake (15–60 min), transferrin labels larger endosomal compartments, possibly recycling endosomes and/or late endosomes. These endosomal compartments show much less Hip1R staining (data not shown). In summary, mHip1R colocalizes with clathrin, AP-2, and with transferrin-labeled early endocytic compartments.

mHip1R Is a Peripheral Membrane Protein that Is Enriched in Clathrin-coated Vesicle Fractions

Since mHip1R colocalized with markers for receptor-mediated endocytosis, it was important to determine whether mHip1R is tightly associated with clathrin-coated vesicles. We first determined by subcellular fractionation whether mHip1R is a soluble or peripheral membrane protein. As shown in Fig. 7 a, the majority of mHip1R associates with the particulate fractions (P1, P2, and P3), and a very small pool is soluble (S3). This distribution is different from that of other cytoskeletal proteins like paxillin and Abp1, but it is very similar to that of clathrin (Fig. 7 and data not shown). mHip1R can be extracted from the particulate fraction with 0.5 M NaCl, indicating that mHip1R is a peripheral membrane protein and not an integral membrane protein (Fig. 7 a, lanes 9 and 10). In addition, extraction of P2 with the nonionic detergent Triton X-100 showed that a pool of mHip1R is Triton X-100–insoluble (Fig. 7 a, lanes 7 and 8), a characteristic shared by many cytoskeletal membrane proteins. These fractionation properties are similar to those of yeast Sla2p and human Hip1 (Kalchman et al., 1997; Wesp et al., 1997).

a **Fractionation** **Extraction of P2**

3000 g   25000 g   175000 g   1% TX-100   0.5 M NaCl

S1 P1   S2 P2   S3 P3   S   P   S   P

Hip1R
Actin
Paxillin
Clathrin

b

S1 P2 S2   S3 P3 S4 V

190 —
120 —
85 —
61 —
50 —
40 —
25 —

— 190
— 120
— 85
— 61
— 50
— 40
— 25

c

S1 P2 S2   S3 P3 S4 V

Clathrin
Hip1R
Eps15
AmphII
Abp1
Bip1
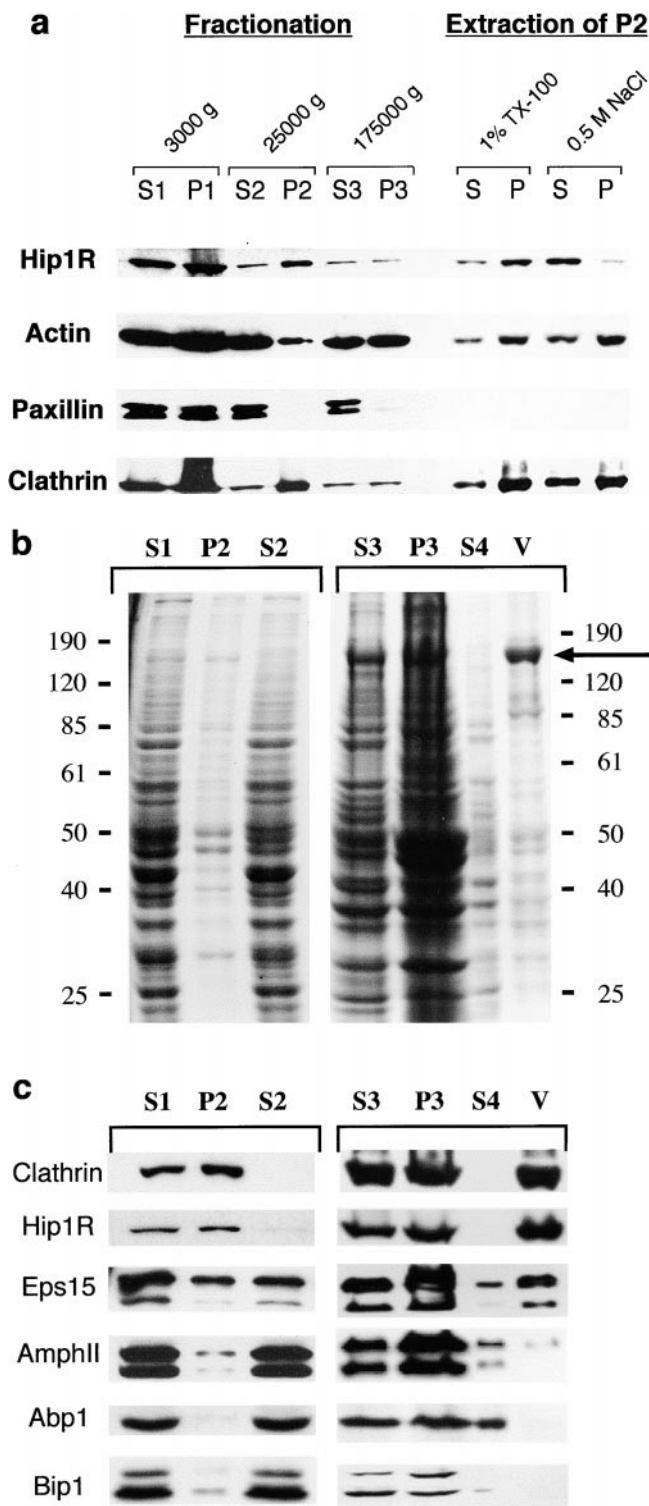
Figure 7. mHip1R is a peripheral membrane protein that cofractionates with clathrin-coated vesicles. (a) Subcellular fractionation of mHip1R. Different fractions of mouse brain homogenate were resolved by SDS-PAGE and examined for the indicated proteins by immunoblotting. The P2 fractions were extracted under different conditions as indicated in the figure. For each pellet (P) and supernatant (S) fraction, equal amounts of protein were loaded. (b and c) Purification of clathrin-coated vesicles from mouse brain homogenate. Fraction (V) represents enriched clathrin-coated vesicles. Equivalent portions of S1, P2, and S2 were loaded (~0.02% of the fraction), and equivalent portions of S3, P3, S4, and V were loaded (~2% of the fraction). (b) Coomassie-stained gel of the fractions. Arrow indicates the band corresponding to the clathrin–heavy chain enriched in the vesicle fraction. (c) Immunoblotting of fractions.

Because the association of mHip1R with P2 and P3 could reflect association with endosomes and vesicles, we next examined whether mHip1R copurifies with clathrin-coated vesicles. Clathrin-coated vesicles were purified from mouse brain, and as shown in Fig. 7 c, mHip1R was highly enriched in this preparation, similar to clathrin. Coomassie staining (Fig. 7 b) shows that clathrin was a major component of this vesicle fraction, and that we achieved a clathrin-coated vesicle purity similar to that described previously in the literature (Lindner, 1998). This fraction contained no detectable levels of BiP1, which is a protein resident in the ER (Fig. 7 c), or any detectable levels of syntaxin 1, which is a protein resident in the plasma membrane (data not shown). Other known components of clathrin-coated vesicles, Eps15 and Amphiphysin 2, were present in this preparation, although they did not appear enriched to the same extent as mHip1R (Fig. 7 c). Other cytoskeletal proteins like mAbp1 and paxillin were not detected in the clathrin-coated vesicle preparation (Fig. 7 c and data not shown).

mHip1R Contains Cytoskeletal and Endocytic Localization Signals

The in vitro actin binding assay and the subcellular fractionation results suggested that mHip1R associates with both the actin cytoskeleton and components of clathrin-coated vesicles. To identify which domain(s) are responsible for these interactions in vivo, we determined the subcellular localization of different mHip1R fragments expressed in COS-7 cells (Fig. 8 a). The fragments were tagged with myc and/or with GFP. Each of these constructs expressed a stable protein that migrated on SDS gels at the predicted molecular weight (Fig. 8 b).

Both mHip1R (aa 1–1068)–GFP and mHip1R (aa 1–1068)–6 myc showed a punctate subcellular localization similar to the endogenous protein (Fig. 8, c and d). In addition, analysis of mHip1R (aa 1–1068)–GFP revealed a localization similar to the endogenous protein at membrane ruffles (data not shown). This analysis was confined to cells expressing lower levels of the tagged proteins, because in cells expressing higher levels, the specific staining is obscured by the increased cytosolic staining. The observed staining patterns and the fact that these full-length constructs colocalized with endogenous clathrin and AP-2 (data not shown) suggested that the tags did not interfere with mHip1R localization.

In contrast to the full-length protein, mHip1R (aa 766–1068)–GFP, which expresses the talin-like domain alone, did not show a punctate staining pattern but instead showed continuous staining enriched at the cell cortex. That mHip1R (aa 766–1068)–GFP colocalized with F-actin is especially evident in membrane ruffles in COS-7 cells (Fig. 8 e). This result is consistent with the in vitro actin binding assay, showing that this talin-like domain copellets with F-actin. This construct also showed some nuclear staining even at low expression levels. mHip1R (aa 346–
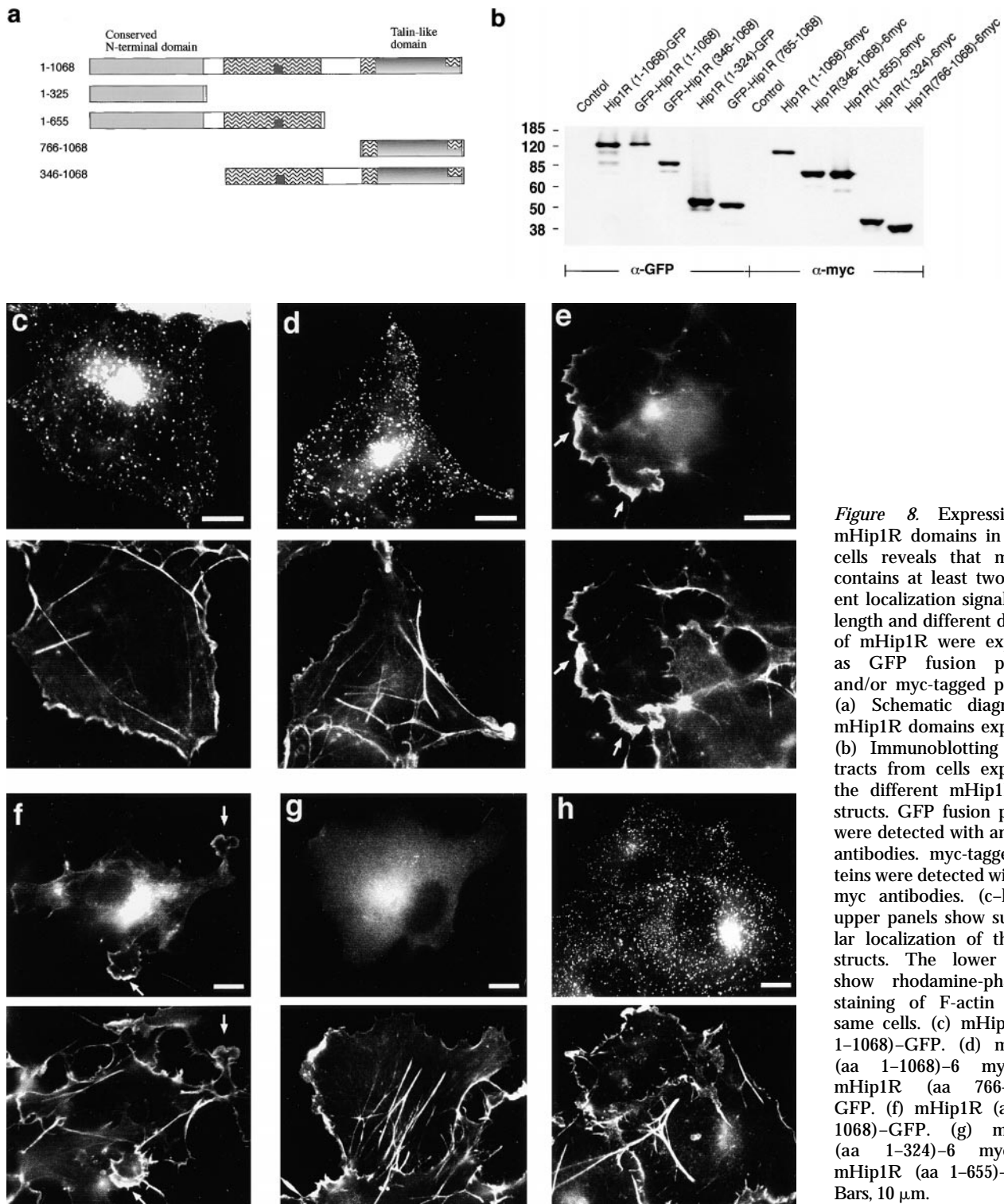
Figure 8. Expression of mHip1R domains in COS-7 cells reveals that mHip1R contains at least two different localization signals. Full-length and different domains of mHip1R were expressed as GFP fusion proteins and/or myc-tagged proteins. (a) Schematic diagram of mHip1R domains expressed. (b) Immunoblotting of extracts from cells expressing the different mHip1R constructs. GFP fusion proteins were detected with anti-GFP antibodies. myc-tagged proteins were detected with anti-myc antibodies. (c–h) The upper panels show subcellular localization of the constructs. The lower panels show rhodamine-phalloidin staining of F-actin in the same cells. (c) mHip1R (aa 1–1068)–GFP. (d) mHip1R (aa 1–1068)–6 myc. (e) mHip1R (aa 766–1068)–GFP. (f) mHip1R (aa 346–1068)–GFP. (g) mHip1R (aa 1–324)–6 myc. (h) mHip1R (aa 1–655)–6 myc. Bars, 10 μm.

1068)–GFP, which expresses the talin-like domain and the central, large coiled–coil domain, showed a similar subcellular distribution to that of the talin-like domain alone, although the cortical staining was less pronounced (Fig. 8 f). mHip1R (aa 766–1068) and mHip1R (aa 346–1068) were also expressed with a 6 myc-tag. These constructs showed a similar distribution to the GFP constructs, but the cortical staining was less pronounced (data not shown). The

NH$_2$-terminal domain (mHip1R [aa 1–324]–6 myc), which in yeast has been shown to be important for endocytosis (Wesp et al., 1997), showed cytosolic staining when expressed with a myc-tag (Fig. 8 g). When expressed as a GFP fusion (mHip1R [aa 1–324]–GFP), this construct also localized to the nucleus (data not shown). In contrast, mHip1R (aa 1–655)–6 myc, which expresses the NH$_2$-terminal domain and the first, central coiled–coil domain,

shows a punctate localization similar to the endogenous protein (Fig. 8 h). This construct also colocalized with clathrin and AP-2 (data not shown). These results show that the talin-like domain is not required for localization with the endocytic machinery.

### Visualization of mHip1R-GFP in Detergent-extracted and Live Cells

Next, we investigated the dynamics of mHip1R in live cells. It has been shown previously that clathrin-coated pits labeled with GFP–clathrin are retained in unfixed, detergent-extracted cells (Gaidarov et al., 1999). To test whether mHip1R-labeled puncta behave like coated pits, we observed mHip1R–GFP in COS-7 cells before and after treatment with Triton X-100. As shown in Fig. 9, a and b, the majority of mHip1R-GFP–labeled puncta at the cell cortex were retained in extracted cells. In contrast, the perinuclear staining and the cytosolic staining were lost upon Triton X-100 treatment. These results are similar to those obtained from studies on GFP–clathrin (Gaidarov et al., 1999). To test whether mHip1R-labeled puncta exhibit dynamic behavior similar to that described previously for GFP–clathrin (Gaidarov et al., 1999), we observed individual puncta at the cell cortex at 1.5-s intervals over 45 frames. During this 67.5-s interval, ~60% of the puncta remained in the same relative location. In contrast, some new puncta appeared, whereas ~40% of the puncta present in the first frame disappeared or were greatly diminished in subsequent images (Fig. 9 c). As with the observations for clathrin-GFP, some puncta disappeared abruptly, whereas others showed a more gradual change in intensity (compare disappearing puncta in Fig. 9).

Given the fact that mHip1R was also present in lamellipodia, we next investigated the dynamics of mHip1R puncta in lamellipodia of motile NIH/3T3 fibroblasts.

Lamellipodia are regions of high membrane and actin dynamics. These regions are relatively flat, thus facilitating the visualization of individual puncta over extended areas of the cell. In these lamellipodia, mHip1R–GFP puncta were observed in addition to some staining at the leading edge (Fig. 10). The majority of these mHip1R–GFP puncta were motile and moved from the leading edge towards the center of the cells (Fig. 10 a). Random movements were rarely observed. These directed movements were not observed in COS-7 cells. However, COS-7 cells do not form any extended lamellipodial protrusions. The motile puncta showed a net rate of movement of ~0.5–3.0 μm/min inward from the cell periphery. The fastest movements were observed within a zone extending ~5 μm in from the cell edge. As shown in Fig. 10 a, puncta further away from the cell edge often appeared to be aligned on linear tracks. These puncta moved slowly inwards at a uniform rate (<1 μm/min). To test whether the movement of the puncta in lamellipodia was dependent on F-actin, we observed individual cells before and after treatment with LAT-A, a monomer-sequestering drug that causes depolymerization of actin filaments (Coué et al., 1987; Spector et al., 1989). Before treatment with LAT-A, individual puncta moved inwards from the cell periphery (Fig. 10 b). 5–10 min after adding LAT-A, these puncta no longer showed net movement away from the cell periphery. They were either stationary or were moving in a random fashion (Fig. 10 c).

Discussion

The actin cytoskeleton has been implicated in endocytosis, yet few direct links between the actin cytoskeleton and the endocytic machinery have been established. Here, we show that mHip1R, a mouse homologue of yeast Sla2p, as-
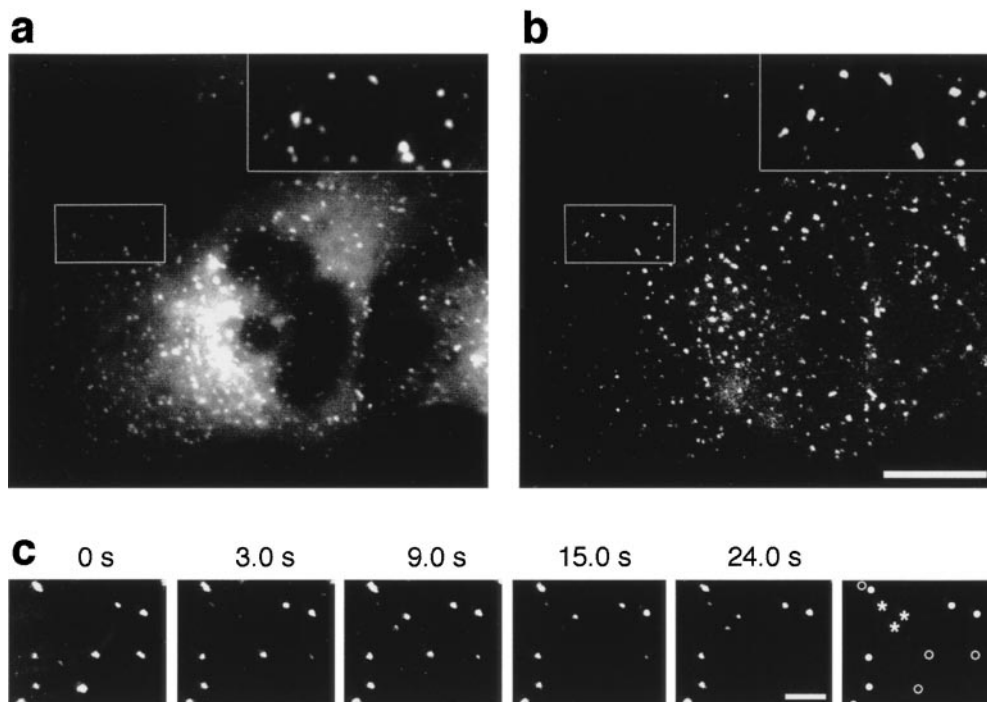
Figure 9. Time-lapse video microscopy of mHip1R–GFP in COS-7 cells. (a and b) The distribution of mHip1R–GFP in a cell before (a) and 45 s after (b) addition of Triton X-100 shows that the cortical staining is retained in extracted cells. Bar, 10 μm. (c) Images at 1.5-s intervals show that mHip1R–GFP puncta exhibit dynamic behavior. Changes in individual mHip1R–GFP puncta throughout this series of images are summarized in the diagram to the right, in which persistent (filled circles), disappearing (open circles), and appearing (asterisks) puncta are indicated. Bar, 2.5 μm.
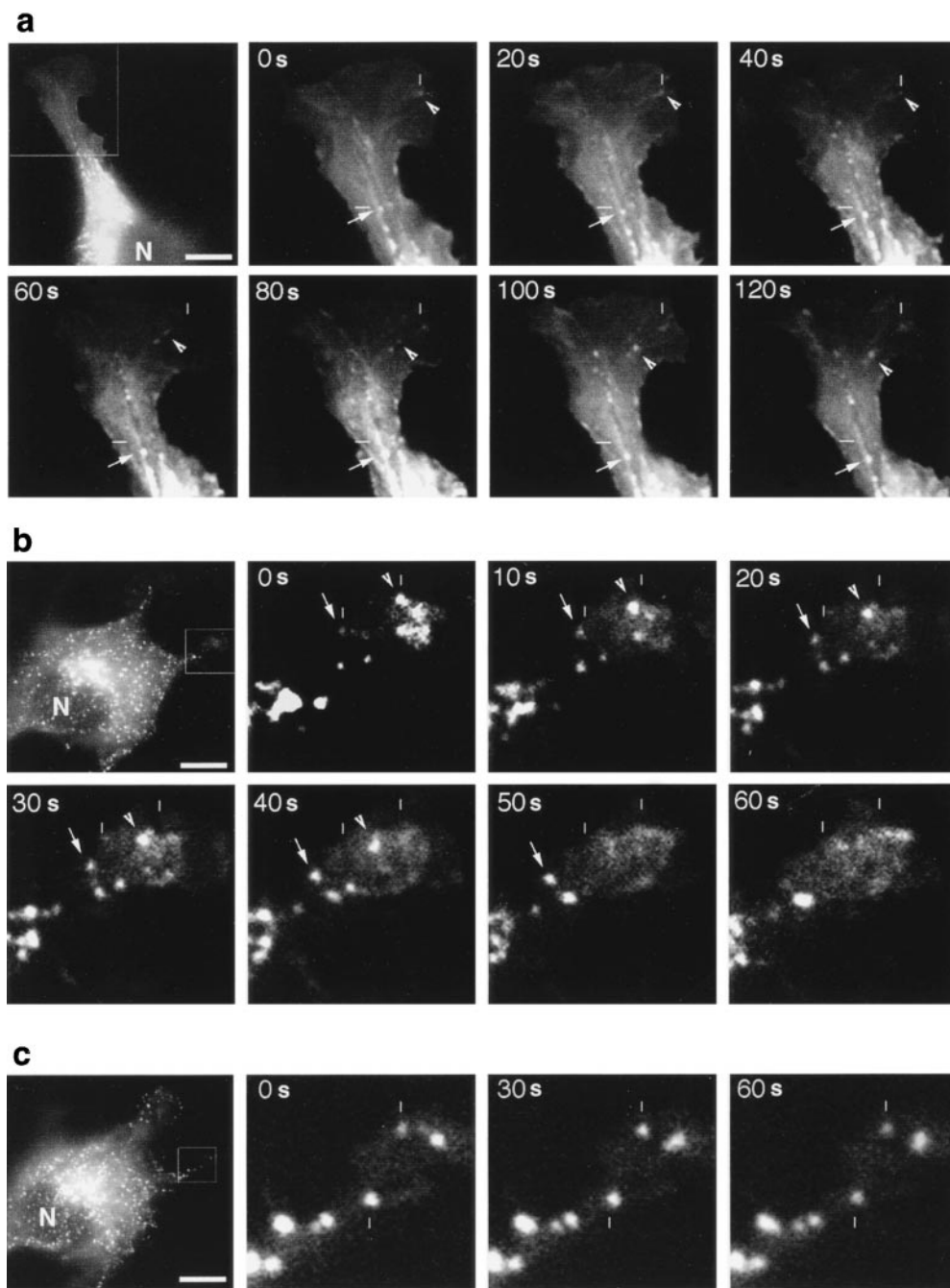
Figure 10. Time-lapse video microscopy of mHip1R–GFP in NIH/3T3 fibroblasts. (a–c) The first image in each series shows a low magnification overview of the cell. Bars in the figures serve as stationary reference points. (a) Images taken at 20-s intervals show movement of mHip1R–GFP away from the cell periphery (see arrows and arrowheads). Puncta further away from the cell periphery often appear to align on linear tracks (see arrows). Bar, 10 μm. (b) Cell before treatment with LAT-A. Puncta are moving inwards from the cell periphery (see arrows and arrowheads). (c) Same cell 5 min after adding LAT-A. The puncta no longer show a net movement away from the cell periphery. Bar, 10 μm.

sociates with both actin filaments and clathrin-coated pits and vesicles.

Sequence alignments and secondary structure predictions clearly show that mHip1R belongs to the Sla2 family of proteins. Furthermore, we suggest that this protein is an ortholog of human Hip1R, because these two proteins show high sequence identity and similar ubiquitous tissue distribution. In contrast, Hip1 is predominantly expressed in the brain (Kalchman et al., 1997).

Our biochemical and colocalization studies demonstrated that mHip1R associates with clathrin-coated vesicles. Since mHip1R colocalized with AP-2 at the cell cortex and shows spatial overlap with transferrin-labeled endocytic compartments at early stages of uptake, we con-

clude that mHip1R is a component of both clathrin-coated vesicles and clathrin-coated pits. In support of the association of mHip1R with clathrin-coated pits, we showed in COS-7 cells that puncta at the cell cortex labeled with mHip1R–GFP exhibit similar behavior to that reported previously for puncta labeled with clathrin–GFP in this cell type (Gaidarov et al., 1999). That is, in both cases the puncta remained relatively stationary, but their signal intensities changed dramatically, with puncta disappearing and appearing over time. Furthermore, the cortical mHip1R staining is resistant to extraction with Triton X-100, a property shared with clathrin–GFP (Gaidarov et al., 1999).

It is interesting that mHip1R is not only enriched at the

cell cortex but also in the perinuclear region, another region of clathrin localization. Clathrin is involved not only in endocytosis but also in budding of exocytic vesicles from the TGN (Robinson, 1987; Ahle et al., 1988). The perinuclear staining of mHip1R is sensitive to treatment with brefeldin A and nocodazole (data not shown), suggesting that this immunostaining represents the TGN. Thus, mHip1R may function both in clathrin-mediated endocytosis and in clathrin-mediated budding from the TGN. Currently, the molecular function of mHip1R in these processes is not known. However, it is important to note that both pathways involve formation of invaginations of membrane, coat assembly, and vesicle fission, processes for which a related machinery is used (for review see Hirst and Robinson, 1998). Not only does the coat contain clathrin in both cases, but the adaptor complexes employed are related (AP-2 at the plasma membrane and AP-1 at the TGN). It is attractive to speculate that mHip1R may be capable of interacting in a similar manner with the related vesicle budding machinery that mediates endocytosis and TGN vesicle budding. It is worth noting that huntingtin protein has also been identified as a component of clathrin-coated vesicles (Velier et al., 1998), suggesting Hip1 and/or Hip1R and huntingtin might function together in clathrin-mediated processes.

mHip1R is a modular protein with several conserved domains that could potentially interact with other proteins. The talin-like domain is the most conserved sequence among Sla2p family members. Here, we showed that this domain of mHip1R binds to F-actin in vitro and colocalizes with F-actin in vivo. This demonstrates that F-actin binding is a conserved activity between mHip1R and yeast Sla2p (McCann and Craig, 1997). Deletion of the talin-like domain in Sla2p has only a subtle effect on actin cytoskeleton organization and does not appear to affect endocytosis, whereas overexpression of this domain causes dramatic defects in actin organization, with an increase in F-actin structures (Wesp et al., 1997; Yang et al., 1999). Yang et al. (1999) concluded that this domain may provide functions redundant with that of the Sla2 NH_2 terminus. More work is required to fully elucidate the function of the mHip1R talin-like domain.

We show that within the NH_2-terminal part of the protein, mHip1R contains a second localization signal that is important for association with the endocytic machinery. The NH_2-terminal domain alone showed a nonvesicular cytosolic and nuclear staining, whereas the NH_2-terminal domain plus the coiled–coil domain localized in a manner similar to the full-length protein. This observation suggests that the central coiled–coil domain contains the signal, or that both domains are needed simultaneously. We favor the latter possibility, because expression of the coiled–coil domain together with the talin-like domain does not show a punctate staining but instead shows colocalization with F-actin. One possibility is that the NH_2-terminal domain plus the central coiled–coil domain dimerizes with the endogenous protein. In yeast Sla2p, the NH_2-terminal domain has been shown to be essential for receptor-mediated endocytosis, whereas other domains are dispensable (Wesp et al., 1997). The NH_2-terminal deletion mutant also had defects in cell morphology and organization of the actin cytoskeleton (Wesp et al., 1997). Interestingly,

Wesp et al. (1997) showed that a mutant lacking the central coiled–coil domain in Sla2p in combination with deletion of either Abp1p or Srv2p, also caused a defect in receptor-mediated endocytosis. *ABP1* and *SRV2* are genes encoding two actin-binding proteins whose null alleles are synthetic lethal with *sla2Δ*, indicating that these proteins may perform redundant functions (Holtzman et al., 1993; Lila and Drubin, 1997). Therefore, we concluded that the NH_2-terminal domain and the central coiled–coil domain are involved in endocytosis, and that the latter domain may be functionally redundant with either Abp1p or Srv2p. This conclusion is consistent with our observation that both the NH_2-terminal domain and the central coiled–coil domain are required for localization to clathrin-coated pits and vesicles.

As discussed above, full-length mHip1R did not show a subcellular localization that is typical of F-actin binding proteins. Instead, it appears to be tightly associated with clathrin-coated vesicles and pits. However, endocytosis occurs at the actin-rich cell cortex. There, membrane-associated mHip1R could bind to the actin cytoskeleton directly. A further indication of the relevance of mHip1R actin association is the fact that the endogenous protein is present in some membrane ruffles, where it partially colocalizes with the actin cytoskeleton. It has been shown previously that depolymerization of the actin cytoskeleton inhibits receptor-mediated endocytosis in some cell types (Gottlieb et al., 1993; Lamaze et al., 1997), and it has been speculated that the actin cytoskeleton may provide a force required for budding and/or provide a scaffold for the endocytic machinery. The function of mHip1R could be to link the actin cytoskeleton to coated pits to facilitate vesicle budding.

The actin cytoskeleton might also be involved in the transport of vesicles away from the plasma membrane. There is evidence that pinocytic vesicles associate with actin tails, and it has been proposed that endocytic vesicles and pinosomes move into the cytosol by means of a brief burst of actin polymerization, analogous to the movement of *Listeria* and *Shigella* (Merrifield et al., 1999). Recently, two proteins that are known to affect actin dynamics have also been shown to associate with components of the endocytic machinery. First, N-WASP, a protein that can stimulate the nucleation activity of the Arp2/3 complex (Rohatgi et al., 1999), has been shown to interact with syndapin I (Qualmann et al., 1999). Syndapin I is an src homology domain 3 (SH3)-containing brain protein that binds to the GTPase dynamin I (Qualmann et al., 1999), the protein that controls the vesicle fission event in receptor-mediated endocytosis (for review see Schmid et al., 1998). Second, profilin, a G-actin binding protein that is important for regulation of actin assembly, has been shown to bind to dynamin 1 in vitro and to colocalize with dynamin I in hippocampal neurons (Witke et al., 1998). Profilin is also capable of binding to inositol phosphates (Witke et al., 1998), leading to the speculation that clustering of phospholipids into local domains of the plasma membrane might be a common mechanism to regulate cortical actin assembly as well as membrane flow. In our study, we presented evidence that mHip1R-containing coated pits and/or vesicles move by an actin-dependent mechanism in NIH/3T3 fibroblasts. Punctate structures la-

beled with mHip1R–GFP moved inward from the cell periphery in lamellipodia, and this directed movement was inhibited by LAT-A. Our data suggest that mHip1R is another component linking the actin cytoskeleton to sites of endocytosis. Therefore, mHip1R is a candidate to facilitate this movement.

In yeast, genetic and biochemical data have suggested that Sla2p, along with Abp1p, Srv2p, and Rvs167p, participate in the early stage of endocytosis (for review see Wendland et al., 1998). Abp1p binds both to Rvs167p and to Srv2p (Freeman et al., 1996; Lila and Drubin, 1997). In addition, *sla2Δ* is synthetic lethal with mutants of the genes encoding each of these proteins (Holtzman et al., 1993; Lila and Drubin, 1997). Rvs167p is related to the mammalian protein amphiphysin, which is a protein known to be involved in receptor-mediated endocytosis (for review see Wigge and McMahon, 1998). Srv2, on the other hand, is a protein implicated in cAMP and Ras signaling (Fedor-Chaiken et al., 1990; Field et al., 1990). Sla2p also has been recently implicated by yeast two-hybrid interactions in signaling to the actin cytoskeleton by binding to the Ser/Thr kinase Ark1p (Cope et al., 1999). Ark1p shows genetic interactions with Prk1p, a homologous kinase, which in turn shows genetic interactions with both Sla2p and Abp1p (Cope et al., 1999). Thus, in yeast a network of physical and genetic interactions involving kinases, cortical actin patch proteins, and components of the endocytic machinery is emerging (Wendland et al., 1998; Cope et al., 1999). For most of these yeast proteins, related proteins in mammals are known. For example, we have recently identified and characterized mAbp1, a mouse protein related to yeast Apb1p (Kessels et al., 2000). Further studies drawing on the complementary experimental advantages of yeast and mammalian cells will provide insights into the molecular role of mHip1R, and will reveal the function of the actin cytoskeleton in endocytosis. These studies may also provide insights into the etiology of Huntington disease.

References

Ahle, S., A. Mann, U. Eichelsbacher, and E. Ungewickell. 1988. Structural relationships between clathrin assembly proteins from the Golgi and the plasma membrane. *EMBO (Eur. Mol. Biol. Organ.) J.* 7:919–929.

Ausubel, F.M., R. Brent, R.E. Kingston, D.D. Moore, J.G. Seidman, J.A. Smith, and K. Struhl. 1994. Current Protocols in Molecular Biology. John Wiley and Sons, New York. 16.7.1–16.7.7.

Ayscough, K.R., J. Stryker, N. Pokala, M. Sanders, P. Crews, and D.G. Drubin. 1997. High rates of actin filament turnover in budding yeast and roles for actin in establishment and maintenance of cell polarity revealed using the actin inhibitor latrunculin-A. *J. Cell Biol.* 137:399–416.

Belmont, L.D., and D.G. Drubin. 1998. The yeast V159N actin mutant reveals roles for actin dynamics in vivo. *J. Cell Biol.* 142:1289–1299.

Bradford, M.M. 1976. A rapid and sensitive method for the quantitation of microgram quantities of protein utilizing the principle of protein-dye binding. *Anal. Biochem.* 72:248–254.

Cope, M.J.T.V., S. Yang, C. Shang, and D.G. Drubin. 1999. Novel protein kinases Ark1p and Prk1p associate with and regulate the cortical actin cytoskeleton in budding yeast. *J. Cell Biol.* 144:1203–1218.

Coué, M., S.L. Brenner, I. Spector, and E.D. Korn. 1987. Inhibition of actin polymerization by latrunculin A. *FEBS Lett.* 213:316–318.

Drubin, D.G., K.G. Miller, and D. Botstein. 1988. Yeast actin-binding proteins: evidence for a role in morphogenesis. *J. Cell Biol.* 107:2551–2561.

Fedor-Chaiken, M., R.J. Deschenes, and J.R. Broach. 1990. SRV2, a gene required for RAS activation of adenylate cyclase in yeast. *Cell.* 61:329–340.

Field, J., A. Vojtek, R. Ballester, G. Bolger, J. Colicelli, K. Ferguson, J. Gerst, T. Kataoka, T. Michaeli, S. Powers, et al. 1990. Cloning and characterization of CAP, the *S. cerevisiae* gene encoding the 70 kd adenylyl cyclase-associated protein. *Cell.* 61:319–327.

Freeman, N.L., T. Lila, K.A. Mintzer, Z. Chen, A.J. Pahk, R. Ren, D.G. Drubin, and J. Field. 1996. A conserved proline-rich region of the *Saccharomyces cerevisiae* cyclase-associated protein binds SH3 domains and modulates cytoskeletal localization. *Mol. Cell. Biol.* 16:548–556.

Gaidarov, I., F. Santini, R.A. Warren, and J.H. Keen. 1999. Spatial control of coated-pit dynamics in living cells. *Nat. Cell Biol.* 1:1–7.

Geli, M.I., and H. Riezman. 1998. Endocytic internalization in yeast and animal cells: similar and different. *J. Cell Sci.* 111:1031–1037.

Goode, B.L., J.J. Wong, A.C. Butty, M. Peter, A.L. McCormack, J.R. Yates, D.G. Drubin, and G. Barnes. 1999. Coronin promotes the rapid assembly and cross-linking of actin filaments and may link the actin and microtubule cytoskeletons in yeast. *J. Cell Biol.* 144:83–98.

Gottlieb, T.A., I.E. Ivanov, M. Adesnik, and D.D. Sabatini. 1993. Actin microfilaments play a critical role in endocytosis at the apical but not the basolateral surface of polarized epithelial cells. *J. Cell Biol.* 120:695–710.

Hirst, J., and M.S. Robinson. 1998. Clathrin and adaptors. *Biochim. Biophys. Acta.* 1404:173–193.

Holtzman, D.A., S. Yang, and D.G. Drubin. 1993. Synthetic-lethal interactions identify two novel genes, SLA1 and SLA2, that control membrane cytoskeleton assembly in *Saccharomyces cerevisiae*. *J. Cell Biol.* 122:635–644.

Ishikawa, K., T. Nagase, M. Suyama, N. Miyajima, A. Tanaka, H. Kotani, N. Nomura, and O. Ohara. 1998. Prediction of the coding sequences of unidentified human genes. X. The complete sequences of 100 new cDNA clones from brain which can code for large proteins in vitro. *DNA Res.* 5:169–176.

Jackman, M.R., W. Shurety, J.A. Ellis, and J.P. Luzio. 1994. Inhibition of apical but not basolateral endocytosis of ricin and folate in Caco-2 cells by cytochalasin D. *J. Cell Sci.* 107:2547–2556.

Kalchman, M.A., H.B. Koide, K. McCutcheon, R.K. Graham, K. Nichol, K. Nishiyama, P. Kazemi-Esfarjani, F.C. Lynn, C. Wellington, M. Metzler, et al. 1997. HIP1, a human homologue of *S. cerevisiae* Sla2p, interacts with membrane-associated huntingtin in the brain. *Nat. Genet.* 16:44–53.

Kessels, M.M., Å.E.Y. Engqvist-Goldstein, and D.G. Drubin. 2000. Association of mouse actin-binding protein 1 (mAbp1/SH3P7), a src kinase target, with dynamic regions of the cortical actin cytoskeleton in response to Rac GTPase activators. *Mol. Biol. Cell.* In press.

Kozminski, K.G., A.A.J. Chen, A. Rodal, and D.G. Drubin. 2000. Functions and functional domains of the GTPase Cdc42p. *Mol. Biol. Cell.* In press.

Kübler, E., and H. Riezman. 1993. Actin and fimbrin are required for the internalization step of endocytosis in yeast. *EMBO (Eur. Mol. Biol. Organ.) J.* 12:2855–2862.

Lamaze, C., T.H. Chuang, L.J. Terlecky, G.M. Bokoch, and S.L. Schmid. 1996. Regulation of receptor-mediated endocytosis by Rho and Rac. *Nature.* 382:177–179.

Lamaze, C., L.M. Fujimoto, H.L. Yin, and S.L. Schmid. 1997. The actin cytoskeleton is required for receptor-mediated endocytosis in mammalian cells. *J. Biol. Chem.* 272:20332–20335.

Lappalainen, P., and D.G. Drubin. 1997. Cofilin promotes rapid actin filament turnover in vivo [published erratum appears in *Nature* 389:211]. *Nature.* 388:78–82.

Lila, T., and D.G. Drubin. 1997. Evidence for physical and functional interactions among two *Saccharomyces cerevisiae* SH3 domain proteins, an adenylyl cyclase-associated protein and the actin cytoskeleton. *Mol. Biol. Cell.* 8:367–385.

Lindner, R. 1998. Purification of clathrin-coated vesicles from bovine brain, liver, and adrenal gland. *In* Cell Biology: A Laboratory Handbook. Vol. 2. J.E. Celis, editor. Academic Press, San Diego, CA. 70–74.

Lupas, A., M. Van Dyke, and J. Stock. 1991. Predicting coiled coils from protein sequences. *Science.* 252:1162–1164.

Marsh, M., and H.T. McMahon. 1999. The structural era of endocytosis. *Science.* 285:215–220.

McCann, R.O., and S.W. Craig. 1997. The I/LWEQ module: a conserved sequence that signifies F-actin binding in functionally diverse proteins from

yeast to mammals. *Proc. Natl. Acad. Sci. USA.* 94:5679–5684.

Merrifield, C.J., S.E. Moss, C. Ballestrem, B.A. Imhof, G. Giese, I. Wunderlich, and W. Almers. 1999. Endocytic vesicles move at the tips of actin tails in cultured mast cells. *Nat. Cell Biol.* 1:72–74.

Mulholland, J., A. Wesp, H. Riezman, and D. Botstein. 1997. Yeast actin cytoskeleton mutants accumulate a new class of Golgi-derived secretory vesicle. *Mol. Biol. Cell.* 8:1481–1499.

Munn, A.L., B.J. Stevenson, M.I. Geli, and H. Riezman. 1995. end5, end6, and end7: mutations that cause actin delocalization and block the internalization step of endocytosis in *Saccharomyces cerevisiae. Mol. Biol. Cell.* 6:1721–1742.

Na, S., M. Hincapie, J.H. McCusker, and J.E. Haber. 1995. MOP2 (SLA2) affects the abundance of the plasma membrane H(+)-ATPase of *Saccharomyces cerevisiae. J. Biol. Chem.* 270:6815–6823.

Peränen, J., M. Rikkonen, M. Hyvönen, and L. Kääräinen. 1996. T7 vectors with a modified T7lac promoter for expression of proteins in *Escherichia coli. Anal. Biochem.* 236:371–373.

Qualmann, B., J. Roos, P.J. DiGregorio, and R.B. Kelly. 1999. Syndapin I, a synaptic dynamin-binding protein that associates with the neural Wiskott-Aldrich syndrome protein. *Mol. Biol. Cell.* 10:501–513.

Raths, S., J. Rohrer, F. Crausaz, and H. Riezman. 1993. end3 and end4: two mutants defective in receptor-mediated and fluid-phase endocytosis in *Saccharomyces cerevisiae. J. Cell Biol.* 120:55–65.

Reddy, P.H., M. Williams, and D.A. Tagle. 1999. Recent advances in understanding the pathogenesis of Huntington's disease. *Trends Neurosci.* 22:248–255.

Riezman, H., P.G. Woodman, G. van Meer, and M. Marsh. 1997. Molecular mechanisms of endocytosis. *Cell.* 91:731–738.

Robinson, M.S. 1987. 100-kD coated vesicle proteins: molecular heterogeneity and intracellular distribution studied with monoclonal antibodies. *J. Cell Biol.* 104:887–895.

Rohatgi, R., L. Ma, H. Miki, M. Lopez, T. Kirchhausen, T. Takenawa, and M.W. Kirschner. 1999. The interaction between N-WASP and the Arp2/3 complex links Cdc42-dependent signals to actin assembly. *Cell.* 97:221–231.

Salisbury, J.L., J.S. Condeelis, and P. Satir. 1980. Role of coated vesicles, microfilaments, and calmodulin in receptor-mediated endocytosis by cultured B lymphoblastoid cells. *J. Cell Biol.* 87:132–141.

Sandvig, K., and B. van Deurs. 1990. Selective modulation of the endocytic uptake of ricin and fluid phase markers without alteration in transferrin endocytosis. *J. Biol. Chem.* 265:6382–6388.

Schmid, S.L., M.A. McNiven, and P. De Camilli. 1998. Dynamin and its partners: a progress report. *Curr. Opin. Cell Biol.* 10:504–512.

Seki, N., M. Muramatsu, S. Sugano, Y. Suzuki, A. Nakagawara, M. Ohhira, A. Hayashi, T. Hori, and T. Saito. 1998. Cloning, expression analysis, and chromosomal localization of HIP1R, an isolog of huntingtin interacting protein (HIP1). *J. Hum. Genet.* 43:268–271.

Spector, I., N.R. Shochet, D. Blasberger, and Y. Kashman. 1989. Latrunculins—novel marine macrolides that disrupt microfilament organization and affect cell growth: I. Comparison with cytochalasin D. *Cell. Motil. Cytoskelet.* 13:127–144.

Velier, J., M. Kim, C. Schwarz, T.W. Kim, E. Sapp, K. Chase, N. Aronin, and M. Difiglia. 1998. Wild-type and mutant huntingtins function in vesicle trafficking in the secretory and endocytic pathways. *Exp. Neurol.* 152:34–40.

Wanker, E.E., C. Rovira, E. Scherzinger, R. Hasenbank, S. Wälter, D. Tait, J. Colicelli, and H. Lehrach. 1997. HIP-I: a huntingtin interacting protein isolated by the yeast two-hybrid system. *Hum. Mol. Genet.* 6:487–495.

Wellington, C.L., R.R. Brinkman, J.R. O'Kusky, and M.R. Hayden. 1997. Toward understanding the molecular pathology of Huntington's disease. *Brain Pathol.* 7:979–1002.

Wendland, B., S.D. Emr, and H. Riezman. 1998. Protein traffic in the yeast endocytic and vacuolar protein sorting pathways. *Curr. Opin. Cell Biol.* 10:513–522.

Wesp, A., L. Hicke, J. Palecek, R. Lombardi, T. Aust, A.L. Munn, and H. Riezman. 1997. End4p/Sla2p interacts with actin-associated proteins for endocytosis in *Saccharomyces cerevisiae. Mol. Biol. Cell.* 8:2291–2306.

Wigge, P., and H.T. McMahon. 1998. The amphiphysin family of proteins and their role in endocytosis at the synapse. *Trends Neurosci.* 21:339–344.

Witke, W., A.V. Podtelejnikov, A. Di Nardo, J.D. Sutherland, C.B. Gurniak, C. Dotti, and M. Mann. 1998. In mouse brain profilin I and profilin II associate with regulators of the endocytic pathway and actin assembly. *EMBO (Eur. Mol. Biol. Organ.) J.* 17:967–976.

Wolkoff, A.W., R.D. Klausner, G. Ashwell, and J. Harford. 1984. Intracellular segregation of asialoglycoproteins and their receptor: a prelysosomal event subsequent to dissociation of the ligand-receptor complex. *J. Cell Biol.* 98:375–381.

Yang, S., M.J.T.V. Cope, and D.G. Drubin. 1999. Sla2p is associated with the yeast cortical actin cytoskeleton via redundant localization signals. *Mol. Biol. Cell.* 10:2265–2283.